RESEARCH PAPER

PCCP
www.rsc.org/pccp

Rotational spectra and structure of the Ar_2–H_2S complex: pulsed nozzle Fourier transform microwave spectroscopic and *ab initio* studies

Pankaj K. Mandal, Dharmender J. Ramdass and E. Arunan*

Department of Inorganic and Physical Chemistry, Indian Institute of Science, Bangalore, 560012, India. E-mail: arunan@ipc.iisc.ernet.in

Received 11th March 2005, Accepted 7th June 2005
First published as an Advance Article on the web 21st June 2005

This paper reports the rotational spectrum and structure of the Ar_2–H_2S complex and its HDS and D_2S isotopomers. The ground state structure has heavy-atom C_{2v} symmetry with the two Ar atoms indistinguishable and H_2S freely rotating as evinced by the fact that asymmetric top energy levels with K_p = odd levels are missing. The rotational constants for the parent isotopomer are: A = 1733.115(1) MHz, B = 1617.6160(5) MHz and C = 830.2951(2) MHz. Unlike the Ar–H_2S complex, the Ar_2–H_2S does not show an anomalous isotopic shift in rotational constants on deuterium substitution. However, the intermolecular potential is still quite floppy, leading to very different centrifugal distortion constants for the three isotopomers. The Ar–Ar and Ar–c.m.(H_2S) distances are determined to be 3.820 Å and 4.105 Å, respectively. The A rotational constants for Ar_2–H_2S/HDS/D_2S isotopomers are very close to each other and to the B constant of free Ar_2, indicating that H_2S does not contribute to the moment of inertia about the a-axis. *Ab initio* calculations at MP2 level with aug-cc-pVQZ basis set lead to an equilibrium C_{2v} minimum structure with the Ar–Ar line perpendicular to the H–H line and the S away from Ar_2. The centrifugal distortion constants, calculated using the *ab initio* force field, are in reasonable agreement with the experimental values. However, they do not show the variation observed for different isotopmers. The binding energy of Ar_2–H_2S has been determined to be 507 cm^{-1} (6.0 kJ mol^{-1}) by CBS extrapolation after correcting for basis set superposition error. Potential energy scans point out that the barrier for internal rotation of H_2S about its b axis is only 10 cm^{-1} and it is below the zero point energy (13.5 cm^{-1}) in this torsional degree of freedom. Internal rotation of H_2S about its a- and c-axes also have small barriers of about 50 cm^{-1} only, suggesting that H_2S is extremely floppy within the complex.

I. Introduction

Weakly bound complexes, bound by van der Waals or hydrogen bonding interactions have attracted enormous interest in the last few decades.[1–3] Coupling of molecular beam techniques with various spectroscopic methods has resulted in a wealth of experimental data on such complexes. Rotational spectroscopic studies have been revolutionized by the development of the Balle–Flygare pulsed nozzle Fourier transform microwave (PNFTMW) spectrometer.[4] Rotational spectra of these complexes can provide direct information about the ground state structure, which is the starting point towards developing intermolecular potential surfaces (IPS). Accurate IPS, in turn, can lead to detailed understanding of intermolecular interactions.

Rare gas (RG)–molecule complexes have found a unique place in this field, starting with the very first report on the PNFTMW spectrometer.[5] These complexes are useful as model systems to study the effect of dispersive and inductive forces in intermolecular interactions. The RG–HX (X = halogen) complexes are particularly intriguing as all of them have the structure as written with the HX interacting with RG through H. This has led Bader to conclude that these are 'hydrogen bonded' complexes,[6] though such a view would not be accepted by many. Recently, Aquilanti and coworkers have reported scattering studies of RG–H_2O[7] and concluded that the interaction in RG–H_2O attains hydrogen bonding character as the RG is changed from He to Xe. Experimental[8] studies on Ar–H_2O complexes show only a small red-shift (1.5 cm^{-1}) in O–H stretching frequency, significantly smaller than what is commonly observed in hydrogen bonded complexes of H_2O. However, today there are many examples of hydrogen bonded complexes showing a blue-shift in X–H stretching frequency.[9] Wategaonkar and coworkers[10] have recently reported theoretical results that predict a 12 cm^{-1} blue shift in O–H stretching frequency for the 'hydrogen bonded' Ar–hydroquinone complex. If hydrogen bonds can have red or blue-shift in stretching frequencies, logic demands that there may be hydrogen bonds with no shift in stretching frequencies.

It has been pointed out that the binding energies of hydrogen bonded complexes of second row hydrides (HCl and H_2S) have significant contribution from dispersive (van der Waals?) forces compared to those of first row hydrides.[11] With the objective of comparing the weakly bound complexes formed by first and second row hydrides, a systematic investigation on Ar_m–$(H_2O)_n$[12–15] and Ar_m–$(H_2S)_n$[14,16] complexes have been reported earlier. This paper reports results on Ar_2–H_2S complex and completes the series Ar_m–H_2X for m up to 3 and X = O and S. The experiments on Ar_2–H_2S were particularly interesting given the results for Ar–H_2S[16] and Ar_3–H_2S.[14] The Ar–H_2S showed an anomalous isotope effect in rotational constants.[16] The rotational constant B for Ar–D_2S is larger than that of the Ar–H_2S complex. To the best of our knowledge, this is the only example in the literature, showing an increase in rotational constant with increase in mass of an isotope. (Imaginary coordinates are observed if the substituted atom is very close to the center of mass such as in N_2O[17] or H_2O–HCl.[18] However, Ar–H_2S does not belong to this category. The substituted atom is more than 1 Å away from the c.m. It turned out to be the result of an extremely floppy

DOI: 10.1039/b503640b

intermolecular potential surface[19] leading to different zero-point averaged ground state geometries for Ar–H_2S and Ar–D_2S). However, Ar_3–H_2S showed a normal isotope effect.[14] What will be the isotope effect on rotational constants for Ar_2–H_2S complex? What would be the ramifications of a floppy IPS on the rotational spectra of Ar_2–H_2S? How, if at all, does the Ar–H_2S distance vary in going from Ar–H_2S to Ar_3–H_2S? These questions are addressed in this work. Rotational spectra for Ar_2–H_2S,/HDS/D_2S isotopomers are reported. In addition, results of *ab initio* calculations are reported at MP2 and CCSD(T) levels of theory with sufficiently large basis sets, up to aug-cc-pVQZ basis set. The theoretical and experimental results are compared and discussed.

Our interest in H_2S complexes is strengthened by another concern. Recently, we defined 'hydrogen bond radii' for all the hydrogen halides, HCN, H_2O and C_2H_2.[20–22] This definition was based on experimental distances in B$\cdots$HX complexes and the electrostatic potential of isolated B.[23] Though not as strong and prevalent as OH groups, SH groups also involve in hydrogen bonding and they are important in the amino-acid cysteine and its derivatives.[24,25] Experimental data on H_2S complexes are relatively scarce compared to the other HX listed above. Hence, systematic investigations on several H_2S complexes are in progress in our laboratory. As argon is typically used as the carrier gas in these studies, identification and assignment of Ar_m–$(H_2S)_n$ complexes are essential to our larger objective. The other H_2S complexes that are currently being investigated are C_2H_4–H_2S,[26] $(H_2S)_2$,[27] H_2O–H_2S,[27] Ar–$(H_2S)_2$[28] and Ar–$(H_2O$–$H_2S)$.[29]

II. Experimental details

The rotational spectra for Ar_2–H_2S and its isotopomers were observed using the Balle-Flygare pulsed nozzle FT microwave spectrometer, fabricated recently in our laboratory.[21] A roots blower (Boc Edwards, EH 250) has been added in between the rotary pump and the diffusion pump. With this arrangement the spectrometer could be operated at 20 Hz, though usually it is operated at about 5 Hz. The Ar_2–H_2S complex was formed through supersonic expansion of Ar gas seeded with 1 to 2% of H_2S. The D_2S or HDS was formed by flowing H_2S through several bubblers placed sequentially and filled with either D_2O or 1 : 1 D_2O/H_2O mixture, respectively. The back pressure was kept typically at 0.6 atm. The diameter of the 900 series valve (General Valve) is 0.8 mm. The optimum microwave pulse was of 2.0 μs duration. Typically 1000 to 2000 shots were averaged to obtain a reasonable signal to noise ratio. The identity of the complexes was established by confirming the presence of H_2S/D_2S/HDS and Ar. No signal was observed without H_2S or when He was used as the carrier gas. The signal appeared again as a few % of Ar was added to the gas mixture in He. All gases were obtained from Bhoruka Gases Ltd and used as supplied: Ar (99.999%), He (99.999%) and H_2S (99.5%). D_2O was obtained from Sigma-Aldrich, 99.96 atom% D.

III. Results and discussions

III.1. Search and assignment

The geometry of the Ar_2–H_2S complex was assumed to be similar to that of Ar_2–H_2O, which is an asymmetric top having a planar structure with C_{2v} symmetry.[13] In all the complexes involving Ar_2 moiety, the Ar–Ar distance is very close to 3.821 Å, which is the same as in Ar_2 dimer.[22,30] It is observed that Ar/HF systems have rotational constants and rotational spectra very similar to Ar/H_2O systems. For example, the rotational constants for Ar_2–H_2O (3383 MHz 1732 MHz and 1145 MHz)[13] and Ar_2–HF (3576 MHz, 1739 MHz, and 1161 MHz) [31] are quite similar. The same resemblance is observed between Ar/HCl and Ar/H_2S systems. This is because of the similarity in masses between HF and H_2O, and HCl and H_2S and their interactions with Ar_n. A search for the $2_{02} \rightarrow 3_{03}$ transition was started from 5925 MHz downwards, as the corresponding transition for Ar_2–HCl occurs at 5924 MHz.[32] It was found soon at 5830.1040 MHz. (However, this approach is not always successful as evinced by the case of C_2H_4–H_2S. The interaction between the HCl and C_2H_4 is significantly stronger than that of H_2S and C_2H_4.[26]) More transitions could be predicted readily and observed. A total of 22 *A*-dipole transitions were observed for Ar_2–H_2S and 21 transitions were observed for both Ar_2–D_2S and Ar_2–HDS. The search for the deuteriated species was straightforward as the rigid rotor prediction from the Ar_2–H_2S constants gave rotational constants very close to the experimental values, unlike for Ar–H_2S. Table 1 contains all the observed transitions along with their residues for all three isotopomers. The observed transitions were fitted to a distorted asymmetric rotor Hamiltonian using the Watson S-reduction[33] in the III^l representation. The fitted parameters and the standard deviations are shown in Table 2 for all three complexes. For Ar_2–H_2S and Ar_2–HDS, rms deviations were $\sim$3 kHz. However, for Ar_2–D_2S the rms deviation was 8.8 kHz, possibly due to the unresolved hyperfine splitting from D atoms. In all these cases, the uncertainties in determining the rotational constants and the centrifugal distortion constants look reasonable. The distortion constants show significant variation with isotopomers (H_2S, HDS and D_2S) compared to the variation observed for Ar_2–H_2O isotopomers.[13] Such dramatic variation in distortion constants has been noted earlier between C_6H_6-H_2S and C_6H_6-D_2S isotopomers.[34] *Ab initio* force field calculations reported later in this paper do predict the distortion constants reasonably well. However, they do not predict the variation observed for the different isotopomers. It certainly is a manifestation of the floppy nature of these complexes having several large amplitude vibrations.

The vibrationally averaged structure has C_{2v} symmetry as all the transitions observed are between states $J_{Kp,Ko}$, which have K_p and K_o either even–even (*ee*) or even–odd (*eo*). Transitions corresponding to *oe*/*oo* levels could not be seen, though they could be predicted accurately. The C_2-axis interchanges the two identical spin zero ($I = 0$) Ar nuclei and it happens to be the '*a*'-axis for the complex. According to nuclear spin statistics, the levels with '*oo*' and '*oe*' will be missing. The same is true for Ar_2–HCl complex as well.[32] For Ar_2–HF and Ar_2–H_2O complexes the C_2 axis is the '*b*'-axis and the '*eo*' and '*oe*' levels have zero statistical weights.

The sensitivity of the spectrometer below 3 GHz was not good enough to get a good S/N ratio. The $0_{00} \rightarrow 1_{01}$ transitions were not observed for –HDS and –D_2S complexes and in the higher *J* transitions the nuclear hyperfine splitting due to D atom(s) could not be resolved. Hence, quadrupole coupling constants could not be determined. Based on the experimental results for Ar–H_2S[16] and Ar_2–H_2O,[13] two sets of transitions were expected for Ar_2–H_2S/D_2S corresponding to the internal rotor/tunneling states involving different spin states of H_2S/D_2S. However, so far even after extensive searches both above and below the observed lines, no transitions could be unambiguously assigned to a second state. As Ar and H_2S have similar masses, it is suspected that several transitions of Ar–$(H_2S)_2$ also occur in the same region. Many transitions have been assigned for Ar–$(H_2S)_2$ now[28] and it is hoped that unambiguous conclusions about internal rotors states of Ar_2–H_2S will emerge. However, for both Ar_3–H_2S and Ar_3–H_2O complexes also, only one state has been found.[14] Our attempts to look for Ar_2–$H_2{}^{34}S$ were not successful either.

III.2. Structure

The fact that '*oo*' and '*oe*' levels are missing also indicates that H_2S undergoes large amplitude internal motion within the complex. If H_2S were to be rigid and symmetrically bound to

Table 1 Observed rotational transitions of Ar_2–H_2S, Ar_2–HDS and Ar_2–D_2S complexes

	Ar_2–H_2S		Ar_2–HDS		Ar_2–D_2S	
Transitions	Observed freq./MHz	Res[a]/kHz	Observed freq./MHz	Res./kHz	Observed freq./MHz	Res./kHz
$0_{00} \rightarrow 1_{01}$	2447.8427	−1.1	—	—	—	—
$1_{01} \rightarrow 2_{02}$	4211.9863	0.6	4200.3178	−0.9	4190.3226	−17.4
$2_{02} \rightarrow 3_{03}$	5830.1040	0.8	5808.8030	−1.9	5790.6443	−10.5
$2_{21} \rightarrow 3_{22}$	7341.3208	0.9	7291.2183	−8.3	7250.9890	−0.4
$3_{03} \rightarrow 4_{04}$	7484.5311	1.2	7455.4795	−0.5	7430.6364	−6.5
$1_{01} \rightarrow 2_{20}$	7614.6752	2.2	7597.6150	0.8	7586.1016	1.9
$2_{20} \rightarrow 3_{21}$	8852.6162	−0.6	8774.4476	1.1	8714.1249	−8.5
$4_{04} \rightarrow 5_{05}$	9143.5875	0.5	9107.9423	−0.4	9077.4039	−2.3
$3_{22} \rightarrow 4_{23}$	9145.6587	1.0	9103.9619	3.4	9070.2738	15.3
$5_{05} \rightarrow 6_{06}$	10802.5295	0.0	10760.4230	0.8	10724.3530	0.0
$4_{23} \rightarrow 5_{24}$	10825.8807	0.0	10782.6017	3.0	10747.0090	15.3
$3_{21} \rightarrow 4_{22}$	11040.3743	−1.4	11001.0151	5.2	10969.1749	9.2
$2_{02} \rightarrow 3_{21}$	12255.3042	0.0	12171.7410	−0.9	12109.8889	−4.3
$6_{06} \rightarrow 7_{07}$	12460.9390	−0.4	12412.3869	1.1	12370.8844	0.4
$5_{24} \rightarrow 6_{25}$	12485.4364	−1.6	12436.2299	0.4	12395.3050	12.0
$4_{22} \rightarrow 5_{23}$	12596.0798	−5.4	12564.6096	−5.2	12537.5096	−1.0
$4_{41} \rightarrow 5_{42}$	13630.5749	−0.8	13503.8280	5.3	13397.2790	9.4
$7_{07} \rightarrow 8_{08}$	14118.7037	−0.2	14063.7115	0.3	14016.8880	2.7
$6_{25} \rightarrow 7_{26}$	14142.7369	−2.3	14087.0097	−0.2	14040.4908	−8.7
$5_{23} \rightarrow 6_{24}$	14180.7909	7.0	14128.7516	−1.6	14084.5128	−14.5
$4_{40} \rightarrow 5_{41}$	14945.3465	0.2	14760.3978	−2.7	14613.1809	−3.6
$8_{08} \rightarrow 9_{09}$	15775.7315	0.7	15714.3046	−0.7	15662.2745	−0.9

[a] Observed − calculated.

Ar_2 (as in Fig. 1), the spin statistics would be similar to that of C_2H_2 and all rotational levels should be present. If it was rigid but not symmetrically bound, the complex could not have a C_2-axis. The rotational constant A for Ar_2–H_2S is 1733.115(1) MHz, which is very close to that of free Ar_2 dimer.[30] For the –HDS and –D_2S complexes, A is within 1–2 MHz of the above value. A rigid structure will have significantly different A for the three complexes. The A rotational constants for Ar_2–H_2S and Ar_2–HDS differ by 4–6 MHz for rigid structures and for Ar_2–D_2S and Ar_2–H_2S, this difference is about 10 MHz. Clearly, the H_2S unit is not contributing to the A rotational constant of the complex. This, again, happens due to the large amplitude internal rotation of H_2S monomer within the complex.

The intermolecular separation can be determined using the following inertial equations. As H_2S does not contribute to the moments about the a axis, it was assumed to be spherical in this analysis:

$$I_a = I(\mathrm{Ar_2}) = mr^2/2 \quad (1)$$

$$I_b = \mu_c R^2 \quad (2)$$

$$I_c = mr^2/2 + \mu_c R^2 \quad (3)$$

Table 2 Fitted rotational constants, centrifugal distortion constants and standard deviations of the fits for Ar_2–H_2S, Ar_2–HDS and Ar_2–D_2S. 'SD' is the standard deviation of the fit and '#' is the number of transitions fitted and Δ is the inertial defect in a.m.u. Å^2

Parameters	Ar_2–H_2S	Ar_2–HDS	Ar_2–D_2S
A/MHz	1733.115 (1)	1734.216 (1)	1735.369 (4)
B/MHz	1617.6160 (5)	1604.3628 (7)	1594.416 (2)
C/MHz	830.2951 (2)	827.0668 (3)	824.176 (1)
d_1/kHz	−2.26 (2)	−1.68 (3)	0.26 (8)
d_2/kHz	2.565 (5)	6.143 (7)	16.22 (2)
D_J/kHz	41.34 (2)	47.99 (4)	66.2 (1)
D_{JK}/kHz	−69.47 (6)	−83.48 (9)	−124.3 (3)
D_K/kHz	31.79 (4)	39.15 (5)	61.2 (2)
SD/kHz	2.1	3.0	8.8
#	22	21	21
Δ (= $I_c - I_a - I_b$)	4.650	4.630	5.002

Here 'm' is the mass of Ar, 'r' is the Ar–Ar-distance, 'R' is the distance between center of masses of H_2S and Ar_2 unit and 'μ_c' is the reduced mass of the complex. The structural parameters 'r' and 'R' and the inertial axis system are defined in Fig. 1. From eqn. (1), using the Ar_2–H_2S rotational constants, the 'r' value comes out to be 3.820 Å, which is almost identical to the Ar–Ar distance in free Ar_2, 3.821 Å. The Ar_2–HDS and Ar_2–D_2S constants give this value as 3.819 Å and 3.818 Å, respectively. Eqn. (2) and (3) lead to 'R' values of 3.620 Å and 3.646 Å respectively for Ar_2–H_2S and it is taken as 3.633 Å. From these results, the distance between the c.m. of the complex and the c.m.(H_2S) is determined to be 2.549 Å. These values also correspond to the Ar–c.m.(H_2S) distances, R_1, of 4.093 Å and 4.116 Å, respectively, giving an average value of 4.105 Å. The R_1 for Ar–H_2S and Ar_3–H_2S are 4.013 Å and 4.112 Å, respectively. Thus, R_1 for Ar_2–H_2S appears to be very close to those of Ar–H_2S and Ar_3–H_2S and lie in between these values. For comparison, Ar_2–D_2S rotational constants lead to 4.052 Å and 4.077 Å for R_1, from eqns. (2) and (3), respectively. The experimental inertial defect is 4.650 a.m.u. Å^2. This large and positive value supports an effectively planar structure for this complex. This, again, is similar to Ar_2–H_2O complex,[13] which has an inertial defect of 3.52 a.m.u. Å^2.

The above structural analysis gives mainly the distances between the three monomers in Ar_2–H_2S. Qualitative information about the orientation of H_2S can be obtained using the rotational constants of the three isotopomers, Ar_2–H_2S/HDS/D_2S. It is qualitative because of the floppy nature of the complex and also the fact that the substituted atoms are H/D. The distance of the substituted atom from the c.m is given by:[35]

$$|r| = \left[\left(\frac{1}{2\mu}\right)(\Delta I_a + \Delta I_b + \Delta I_c)\right]^{1/2} \quad (4)$$

Here μ is the reduced mass for substitution, $M\Delta m/(M + \Delta m)$. The distances for the two hydrogens are determined to be 1.547 Å and 1.401 Å. These distances may be contrasted with the results from C_2H_4-H_2S complex.[26] It is a very floppy complex as well, with both C_2H_4 and H_2S exhibiting large amplitude motions within the complex. A similar substitution analysis led

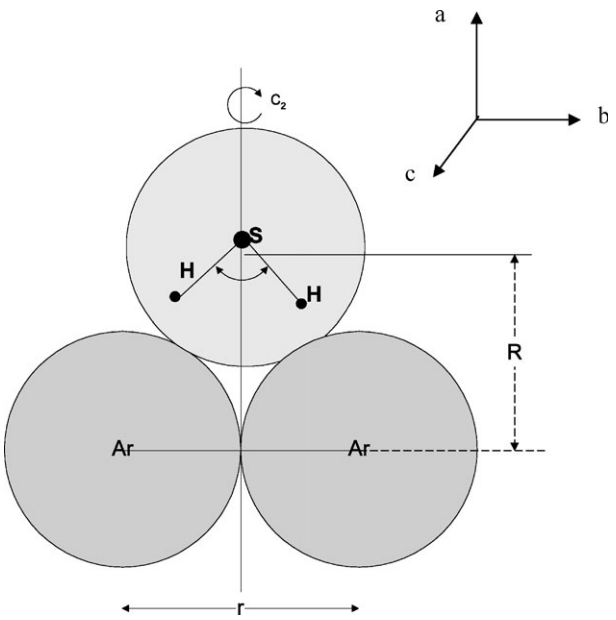

Fig. 1 Experimentally observed, vibrationally averaged geometry of Ar_2–H_2S. The H_2S orientation can not be determined accurately with the experimental data and so a sphere is shown around H_2S. *R* is the distance between the centers of masses of H_2S and Ar_2. *r* is the Ar–Ar distance.

to distances of 1.034 Å and 2.163 Å, clearly indicating that only one hydrogen is pointing towards the π center in C_2H_4.[26] It appears that, in Ar_2–H_2S both hydrogens of H_2S are pointing towards Ar_2. It is also consistent with the distance c.m.(Ar_2–H_2S)–c.m.(H_2S) from the inertial analysis (2.549 Å) reported above. The orientation of H_2S can not be determined any more accurately with the experimental data presented here and hence Fig. 1 shows a sphere around H_2S. All the structural parameters including inertial defects (Δ) for Ar_2–H_2S are given in Table 3 along with results from *ab initio* calculations, which are discussed next.

III.3. *Ab initio* calculations

III.3.a. Geometry. The *ab initio* calculations were done to determine the optimized geometry and the barriers to internal rotation of H_2S within the complex. In addition, the stabilization energy for Ar_2–H_2S was determined using super-molecule approach. Gaussian 98 software package[36] and PC-GAMESS[37] were used for calculations. Frequency calculations were done to ascertain the nature of the stationary points. The vibrational force field from the PC-GAMESS calculations were also used to estimate the centrifugal distortion constants using FCONV/VIBCA codes available through the PROSPE data base.[38] The optimization was done using MP2 method with reasonably large basis sets from 6-311++G** to aug-cc-pVQZ. All calculations resulted in a true minimum with all positive eigenvalues in the Hessian except for the calculation with aug-cc-pVDZ basis set, which resulted in a second-order saddle point. Further, CCSD(T) single point energy calculations were done for all MP2 optimized geometries (except aug-cc-pVQZ) using the same basis set that was used for optimization. The initial geometry for optimization was given as a planar C_{2v} symmetric structure. However, optimization with the different basis sets used in this work led to a non-planar geometry with C_{2v} symmetry as shown in Fig. 2. Both hydrogen atoms are pointing towards the Ar atoms and the S is away from them. Calculations at MP2/6-311++G** level led to another minimum having one H pointing towards Ar_2 and another pointing away.[29] However, this structure could not be optimized with the larger basis sets. Besides, BSSE corrections at this level led to 'de-stabilization' and clearly 6-311++G** basis set is far from adequate for these weakly bound complexes.

The Ar–Ar and Ar–c.m.(H_2S) distances both reduce with increasing basis size. The distances calculated at MP2/6-311++G(3df,2p) are fortuitously close to the experimental values. Particularly, the Ar–Ar distance calculated at this level (3.820 Å) is very close to the R_0 for Ar_2 dimer[30], 3.822(2) Å. However, the R_e for Ar_2 is less at 3.763 Å,[30] and not surprisingly, higher basis sets give better agreement. The structural parameters do show some convergence and the basis sets used, appear to be large enough. It is evident from the theoretical stabilization energies as well and they are discussed next.

III.3.b. Interaction energy and barrier energies for internal rotation. The interaction energy has been calculated at all levels of theory employed in this work using the super-molecule approach.

$$\Delta E = E_{\text{complex}} - E_{\text{Ar}} - E_{\text{Ar}} - E_{\text{H}_2\text{S}} \quad (5)$$

The interaction energy from eqn. (5) needs to be corrected for both the zero point energy (ZPE) differences between the complex and monomers and the basis set superposition error (BSSE).[39] Frequency calculations were done at all basis sets except aug-cc-pVQZ and ZPE corrections were done. The BSSE was calculated using the counterpoise (CP) method as follows:[40,41]

$$\begin{aligned}\text{BSSE} = &[E_{\text{Ar}_1}{}^*(M) + E_{\text{Ar}_2}{}^*(M) + E_{\text{H}_2\text{S}}{}^*(M)] \\ &- [E_{\text{Ar}_1}{}^*(C) + E_{\text{Ar}_2}{}^*(C) + E_{\text{H}_2\text{S}}{}^*(C)] \quad (6)\end{aligned}$$

Here *M* stands for monomer basis sets and *C* stands for complex basis sets and the * denotes that the geometry of the monomer is given as found in the complex. The BSSE corrected interaction energy is given by:

$$\Delta E^{\text{CP}} = \Delta E + \text{BSSE} \quad (7)$$

Usually, the CP corrected interaction energy is given as:[11]

$$\Delta E^{\text{CP}} = E_{\text{complex}} - E_{\text{Ar}_1}{}^*(C) - E_{\text{Ar}_2}{}^*(C) - E_{\text{H}_2\text{S}}{}^*(C) \quad (8)$$

According to eqn. (8),

$$\begin{aligned}\text{BSSE} = &[E_{\text{Ar}_1}(M) + E_{\text{Ar}_2}(M) + E_{\text{H}_2\text{S}}(M)] - [E_{\text{Ar}_1}{}^*(C) \\ &+ E_{\text{Ar}_2}{}^*(C) + E_{\text{H}_2\text{S}}{}^*(C)] \quad (9)\end{aligned}$$

Table 3 The structural parameters for Ar_2–H_2S obtained from different levels of theory and experiment. The distances are given in Å and the inertial defects are given in a.m.u. Å^2

Parameters[a]	6-311++G**	6-311++G (3df,2p)	6-311++G (3df,3pd)	aug-cc-pVDZ	aug-cc-pVTZ	aug-cc-pVQZ	Expt
R	3.584	3.625	3.559	3.638	3.507	3.487	3.633
r	4.064	3.820	3.816	3.882	3.743	3.730	3.820
R_1	4.120	4.097	4.038	4.123	3.975	3.954	4.105
$\Delta(= I_c - I_a - I_b)$	−3.7	−3.8	−3.7	−3.8	−3.8	−3.8	4.7

[a] *R* is the distance between the c.m. of Ar_2 and the c.m.(H_2S); *r* is the Ar–Ar distance; R_1 is the distance between Ar and c.m.(H_2S). Results with 6-311++G(3df,3pd) basis set is from GAMESS calculations and all the others are from Gaussian.

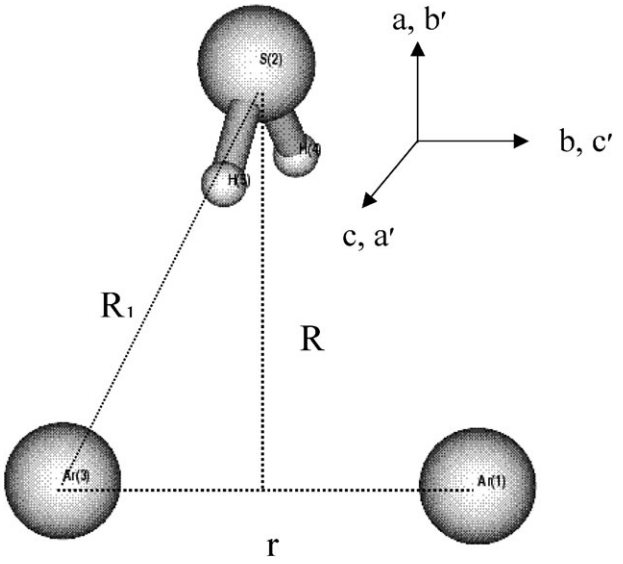

Fig. 2 Optimized structure of Ar_2–H_2S at the MP2/6-311++G(3df,2p) level of theory. The C_{2v} symmetry structure has H_2S plane perpendicular to the Ar–Ar bond. The inertial axes are shown and the prime indicates the axes for H_2S monomer. R is the distance between the centers of masses of H_2S and Ar_2; r is the Ar–Ar distance; and R_1 is the distance between Ar and c.m.(H_2S).

The BSSE calculated from eqns. (6) and (9) will be significantly different, if the monomer geometries are distorted on complex formation. It is important for hydrogen bonded complexes of HF and H_2O, for instance.[42] For the Ar_2–H_2S complex, the difference in BSSE calculated between eqns. (6) and (9), is only 0.5 cm^{-1} at MP2/6-311++G** level calculations. In any case, in this work, BSSE has been reported using eqn. (6) only.

Table 4 shows the interaction energies calculated at MP2 and CCSD(T) level calculations with various basis sets. The BSSE is significant (394 cm^{-1}) at MP2 level with 6-311++G** basis set and in fact it is larger than the absolute value of interaction energy (−348 cm^{-1}), leading to net 'destabilization'. It is interesting to note that single point calculations at CCSD(T) level with this small basis set, increases both ΔE (−354 cm^{-1}) and BSSE (408 cm^{-1}). As the increase in BSSE is more than that of ΔE, the results look worse at CCSD(T) level than at MP2 level. As the basis size is increased to 6-311++G(3df,2p), ΔE increases and BSSE reduces by more than half, leading to a net stabilization of −263 cm^{-1}. As the basis size is increased to aug-cc-pVQZ, the BSSE reduces to 70 cm^{-1} only, ~15% of the interaction energy of −471.1 cm^{-1}. The ZPE correction increased from 103 cm^{-1} with 6-311++G (3df,2p) basis set to 117 cm^{-1} with aug-cc-pVTZ basis set. This increase could be due to the over-estimation of intermolecular vibrational frequencies and it appears that these frequencies should be scaled by 0.7, see next section. The stabilization energy calculated at MP2 level calculations with aug-cc-pVDZ/pVTZ/pVQZ were used to extrapolate to CBS limit.[43] At this limit, the binding energy of Ar_2–H_2S is 507 cm^{-1} and 418 cm^{-1}, respectively without and with ZPE corrections.

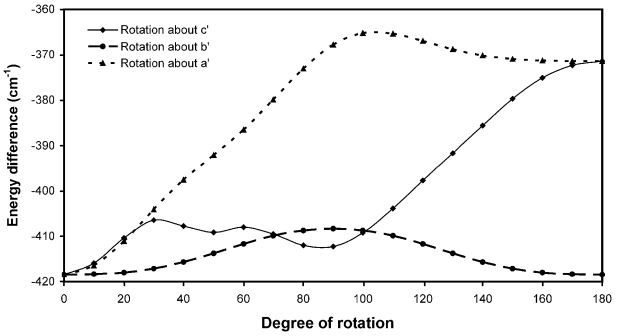

Fig. 3 Potential energy surface scan at MP2/6-311++G(3df,2p) level for internal rotation of H_2S about its inertial axes within the Ar_2–H_2S complex. The S was held fixed in the calculations.

As discussed in the previous section, experimental results do indicate that the H_2S is quite floppy within the complex. Hence, it was decided to determine the barriers for internal rotation of H_2S about its principal axes, within the complex by doing potential energy scans. Energies were calculated by varying the corresponding angles by 10° every step, keeping the other structural parameters fixed. To simplify the calculations, S was held fixed. The results of MP2/6-311++G(3df,2p) calculations are shown in Fig. 3. Not surprisingly, internal rotation about the b axis of H_2S has the lowest barrier of only 10 cm^{-1}. It is less than the zero point energy along this torsional coordinate (13.5 cm^{-1}). The barrier for rotation about a and c axes are also small, 53 and 47 cm^{-1}, respectively. The corresponding torsional frequencies are 49 and 43 cm^{-1}, respectively. It is clear that the H_2S can exhibit very large amplitude motions within the complex.

III.3.c. Vibrational frequencies and centrifugal distortion constants. The vibrational frequencies calculated at MP2/6-311++G(3df,2p) and MP2/aug-cc-pVTZ levels of theory are given in Table 5. The only experimental result available for comparison is that of Ar–Ar stretching observed in the free Ar_2 dimer,[30] which is 30.68 cm^{-1}. It is predicted to be 26 cm^{-1} in Ar_2–H_2S, which seems reasonable. A more stringent test would be the comparison of centrifugal distortion constants from this *ab initio* force field with the experimental values. Kisiel and coworkers[44] have carried out such analysis for Ar_2–HF/HCl/HBr and a similar analysis was done here for Ar_2–H_2S. The FCONV/VIBCA codes were used to determine the centrifugal distortion constants from the *ab initio* force field. Table 6 gives the centrifugal distortion constants and the harmonic vibration-rotation contribution to the inertial defect, determined from the force field with and without scaling. (It should be remembered that the equilibrium inertial defect from the calculations (see Table 3) is about −3.8 a.m.u. Å^2, as the out of plane protons do contribute in the equilibrium structure.

Table 4 The interaction energies obtained from *ab initio* calculations.[a] The values are in cm^{-1}

Energy	6-311++G**		6-311++G(3df,2p)		aug-cc-pVDZ		aug-cc-pVTZ		aug-cc-pVQZ	CBS
	MP2	CCSD(T)	MP2	CCSD(T)	MP2	CCSD(T)	MP2	CCSD(T)	MP2	MP2
ΔE	−347.7	−353.6	−418.3	−364.3	−393.4	−352.0	−484.1	−421.5	−471.1	—
ΔE^{CP}	46.2	54.3	−263.0	−197.9	−242.4	−188.7	−350.9	−290.9	−401.1	−507.1
ΔE^{ZPE}	181.9	190.0	−159.8	−94.7	−125.1[b]	−71.4[b]	−233.6	−173.6	−283.8[b]	−418.2
BSSE	394.2	407.9	155.3	166.3	151.0	163.3	133.2	130.6	70.0	—

[a] BSSE = $[E_{Ar_1}^*(M) + E_{Ar_2}^*(M) + E_{H_2S}^*(M)] - [E_{Ar_1}^*(C) + E_{Ar_2}^*(C) + E_{H_2S}^*(C)]$; see text for details; ΔE^{ZPE} is the interaction energy after zero-point vibrational energy correction over ΔE^{CP}. CBS extrapolation was done using the aug-cc-pVnZ results (ref. 43). [b] Zero point energy corrections used vibrational frequencies calculated at MP2/ aug-cc-pVTZ level.

Table 5 All the vibrational frequencies (in cm^{-1}) of Ar_2–H_2S, bending and stretching frequencies of H_2S in H_2S-H_2S (both H-bond donor and acceptor) and free H_2S, calculated at the MP2 level of theory

	MP2/6-311++G(3df,2p)			MP2/aug-cc-pVTZ		
Vibrational modes	Ar_2–H_2S	H_2S-H_2S[a]	H_2S	Ar_2–H_2S	H_2S-H_2S[a]	H_2S
Intermolecular bending	26	—	—	32	—	—
Intermolecular stretching (Ar–Ar)	26	—	—	26	—	—
Torsion about '*b*'-axis of H_2S	27	—	—	19	—	—
Intermolecular stretching (Ar_2–H_2S)	37	—	—	45	—	—
Torsion about '*c*'-axis of H_2S	43	—	—	43	—	—
Torsion about '*a*'-axis of H_2S	49	—	—	63	—	—
H–S–H bending	1214	1223/1215	1217	1209	1216/1209	1212
S–H symmetric stretch	2776	2741/2773	2776	2773	2729/2769	2771
S–H asymmetric stretch	2794	2786/2792	2795	2792	2783/2789	2791

[a] First entry is for the donor H_2S and the second entry is for acceptor H_2S.

Table 6 Distortion constants (in kHz) and inertial defects[a] (in a.m.u. $Å^2$) from experiment and *ab initio* force field

Distortion constants	Experiment	MP2/6-311++G(3df,3pd)		MP2/aug-cc-pVTZ	
Frequency scaling factor	1.0	1.0	0.7	1.0	0.7
d_1	−2.26 (2)	3.14	6.29	3.74	7.49
d_2	2.565 (5)	−0.91	−1.81	−0.80	−1.60
D_J	41.34 (2)	19.09	38.17	20.15	40.30
D_{JK}	−69.47 (6)	−31.35	−62.69	−32.87	−65.74
D_K	31.79 (4)	13.95	27.89	14.53	29.05
δI_a	—	−1.835	−2.595	−1.582	−2.237
δI_b	—	−1.735	−2.454	−1.667	−2.358
δI_c	—	−0.708	−1.002	−0.497	−0.703
Δ	4.650	2.862	4.047	2.751	3.891

[a] Harmonic vibration-rotation contribution to inertial defect, defined as $I_\alpha = (I_0)_\alpha - \delta I\alpha$.

In Table 6, it has been assumed to be zero as the H_2S appears to be nearly spherical in the complex). A frequency scaling factor of 0.7 gives a reasonable agreement for three of the five distortion constants (D_J, D_{JK} and D_K). The other two constants (d_1 and d_2) are of smaller magnitude in comparison. They are predicted to be of the right order of magnitude but wrong signs. For Ar_2–HBr and Ar_2–HCl, Kisiel and coworkers found that a frequency scaling factor of 0.8 works better. Though, the scaling improves the agreement with centrifugal distortion constants, it is obvious that the Ar–Ar stretching frequency would become even smaller. However, this appears to be a general trend with Ar_2–HX clusters as this frequency is estimated to be 21 cm^{-1}, 24 cm^{-1} and 23 cm^{-1} for Ar_2–HCl,[45] Ar_2–OCS[46] and Ar_2–N_2O[47] by analyzing the respective centrifugal distortion constants.

Despite the reasonable agreement between the experimental centrifugal distortion constants and those derived from a scaled *ab initio* force field, there are at least two experimental observations that point to the inadequacy of the *ab initio* force field. (1) The distortion constants for Ar_2–HDS and Ar_2–D_2S are predicted to be very similar to those of Ar_2–H_2S (within 5%). Experimental distortion constants (see Table 2) for the three isotopomers vary by 60–70%. (2) The inertial defect calculated from the harmonic vibration–rotation contribution is 4.047/3.891 a.m.u. $Å^2$ with 6-311++G(3df,2pd) and aug-cc-pVTZ basis sets, compared to the experimental value of 4.650 a.m.u. $Å^2$. In comparison, for Ar_2–HF/HCl/HBr Kisiel and coworkers[44] found much better agreement between the experimental inertial defect and that calculated from the harmonic vibration-rotation contribution at MP2/aug-cc-pVDZ calculations. These observations highlight the fact that the IPS for Ar_2–H_2S is floppier than the IPS for the relatively strongly bound Ar_2–HX systems. It is hoped that the experimental results reported in this paper would stimulate development of more accurate IPS for Rg-H_2S complexes.

In the Introduction, we commented about the shift in vibrational frequencies observed following complex formation. Table 5 compares the intra-molecular vibrational frequencies involving H_2S for Ar_2–H_2S, H_2S–H_2S, and free H_2S, as well. The S–H stretching frequencies calculated for Ar_2–H_2S are both within 2 cm^{-1} of those corresponding to free H_2S. At the MP2/6-311++G(3df,2p) level, there is a 1 cm^{-1} red shift and at MP2/aug-cc-pVTZ level there is a 1–2 cm^{-1} blue shift. These results suggest that one needs to exercise caution in interpreting small blue shifts. Interestingly, the S–H stretching frequencies calculated for the acceptor H_2S in $(H_2S)_2$ show a red shift of 2–3 cm^{-1} compared to the monomer values. The stretching frequency for donor H_2S in $(H_2S)_2$ shows a red shift of 42 cm^{-1}. For comparison, the red shift observed in OH stretching frequency[48] for the strongly hydrogen bonded $(H_2O)_2$ is significantly higher at 226 cm^{-1}. From the vibrational frequency shifts observed, $(H_2S)_2$ could easily be classified as a hydrogen bonded complex. However, the same can not be concluded about Ar–H_2O (1.5 cm^{-1} red shift)[8] or Ar–H_2S complex. Considering Aquilanti *et al.*'s recent work on Rg–H_2O complexes,[7] it may be expected that the frequency shifts observed in Rg–H_2O and Rg–H_2S would be more pronounced as Rg is changed from He to Xe.

IV. Conclusions

The rotational spectra for Ar_2–H_2S and its isotopomers have been observed using PNFTMW spectrometer. It exhibits normal isotope effect unlike Ar–H_2S dimer. Again, unlike Ar–H_2S, only one set of transitions has been observed. The experimental rotational constants are consistent with a vibrationally averaged heavy-atom C_{2v} symmetric structure with both hydrogen atoms pointing towards Ar_2. The Ar–Ar and Ar–H_2S distances are determined to be 3.820 Å and 4.105 Å, respectively. The Ar–H_2S distance falls in between those determined for Ar–H_2S

dimer (4.013 Å) and Ar_3–H_2S tetramer (4.112 Å). *Ab initio* calculations have also been reported at MP2 and CCSD(T) levels with large basis sets up to aug-cc-pVQZ. MP2 results give a minimum energy structure which is non-planar with C_{2v} symmetry where H_2S plane is perpendicular to the Ar–Ar bond and both hydrogens are pointing towards Ar_2. The CBS extrapolation for binding energy of this complex is about 6 kJ mol^{-1}. The vibrational force field from *ab initio* calculations could reasonably reproduce the experimental centrifugal distortion constants for the parent isotopomer, but they do not predict the changes on D substitution. The harmonic–vibration–rotation contribution to the inertial defect is significantly below the experimental inertial defect, unlike that of Ar_2–HX (X = F,Cl and Br).

Acknowledgements

The authors thank Department of Science and Technology, New Delhi, India for a generous grant and the Director of Indian Institute of Science, Bangalore, India for partial support. We thank A. P. Tiwari and P. C. Mathias for their help in building the spectrometer. Partial support from Council of Scientific and Industrial Research, India is acknowledged. We thank Ankit Jain, KVPY summer fellow, for modifying ASYM82 (see ref. 33) code, Mausumi Goswami for help in experiments and B. Raghavendra for discussions on BSSE calculations. We thank Prof. Z. Kisiel for the FCONV/VIBCA codes from the PROSPE database and also for very helpful discussions.

References

1 van der Waals molecules-I, Special issue, *Chem. Rev*., 1988, **88**(6).
2 van der Waals molecules-II, Special issue, *Chem. Rev*., 1994, **94**(7).
3 van der Waals molecules-III, Special issue, *Chem. Rev*., 2000, **100**(11).
4 T. J. Balle and W. H. Flygare, *Rev. Sci. Instrum*., 1981, **52**, 33.
5 T. J. Balle, E. J. Campbell, M. R. Keenan and W. H. Flygare, *J. Chem. Phys*., 1979, **71**, 2723.
6 R. F. W. Bader, *Atoms in Molecule. A Quantum Theory*, Clarendon Press, Oxford, 1990, p. 302.
7 V. Aquilanti, E. Cornicchi, M. M. Teixidor, N. Saendig, F. Pirani and D. Cappelletti, *Angew. Chem., Int. Ed*., 2005, **44**, 2356.
8 R. Lascola and D. J. Nesbitt, *J. Chem. Phys*., 1991, **95**, 7917.
9 P. Hobza and Z. Havlas, *Chem. Rev*., 2000, **100**, 4253.
10 P. S. Meenakshi, N. Biswas and S. J. Wategaonkar, *J. Chem. Phys*., 2003, **118**, 9963.
11 S. Scheiner, *Hydrogen Bonding, A Theoretical Perspective*, Oxford University Press, New York, 1997, p. 24.
12 E. Arunan, T. Emilsson and H. S. Gutowsky, *J. Am. Chem. Soc*., 1994, **116**, 8418.
13 E. Arunan, C. E. Dykstra, T. Emilsson and H. S. Gutowsky, *J. Chem. Phys*., 1996, **105**, 8495.
14 E. Arunan, T. Emilsson, H. S. Gutowsky and C. E. Dykstra, *J. Chem. Phys*., 2001, **114**, 1242.
15 E. Arunan, T. Emilsson and H. S. Gutowsky, *J. Chem. Phys*., 2002, **116**, 4886.
16 H. S. Gutowsky, T. Emilsson and E. Arunan, *J. Chem. Phys*., 1997, **106**, 5309.
17 C. H. Townes and A. L. Schawlow, *Microwave Spectroscopy*, McGraw Hill, New York, 1955.
18 Z. Kisiel, B. A. Pietrewicz, P. W. Fowler, A. C. Legon and E. Steiner, *J. Phys. Chem. A*, 2000, **104**, 6970.
19 G. de Oliveira and C. E. Dykstra, *J. Chem. Phys*., 1997, **106**, 5316.
20 P. K. Mandal and E. Arunan, *J. Chem. Phys*., 2001, **114**, 3880.
21 E. Arunan, A. P. Tiwari, P. K. Mandal and P. C. Mathias, *Curr. Sci*., 2002, **82**, 533.
22 E. Arunan, S. Dev and P. K. Mandal, *Appl. Spec. Rev*., 2004, **39**, 131.
23 S. R. Gadre and P. K. Bhadane, *J. Chem. Phys*., 1997, **107**, 5625.
24 G. R. Desiraju and T. Steiner, *The Weak Hydrogen Bond: In Structural Chemistry and Biology*, Oxford University Press, Oxford, 1999.
25 G. A. Jeffrey and W. Saenger, *Hydrogen Bonding in Biological Structures*, Springer Verlag, Berlin, 1991.
26 M. Goswami, P. K. Mandal, D. Ramdass and E. Arunan, *Chem. Phys. Lett*., 2004, **393**, 22.
27 F. J. Lovas, unpublished results, private communication. For the $(H_2S)_2$ and (H_2S)–(H_2O) complexes, some new sets of transitions have been observed and analysis is in progress.
28 P. K. Mandal, M. Goswami and E. Arunan, Preliminary results presented at the 60th International Symposium on Molecular Spectroscopy, Columbus, OH, Abstract No: RH07, 2005.
29 P. K. Mandal, PhD Thesis, Indian Institute of Science, Bangalore, 2005.
30 P. R. Herman, P. E. LaRoucque and B. P. Stoicheff, *J. Chem. Phys*., 1988, **89**, 4535.
31 H. S. Gutowsky, T. D. Klots, C. Chuang, C. A. Schmuttenmaer and T. Emilsson, *J. Chem. Phys*., 1986, **86**, 569.
32 T. D. Klots, C. Chuang, R. S. Ruoff, T. Emilsson and H. S. Gutowsky, *J. Chem. Phys*., 1987, **86**, 5315.
33 J. K. G. Watson, in *Vibrational Spectra and Structure*, ed. J. R. Durig, Elsevier, Amsterdam, 1977, **6**, p. 1. We thank G. T. Fraser for providing us with the program ASYM82 by A. G. Maki which was used in the fitting. Ankit Jain added a feature that enables the program to remove one line from the fitting at a time and compare the rms deviation with the full fitting. It is helpful in identifying a wrong assignment.
34 E. Arunan, T. Emilsson, H. S. Gutowsky, G. T. Fraser, G. de Oliveira and C. E. Dykstra, *J. Chem. Phys*., 2002, **117**, 9766.
35 W. Gordy and R. L. Cook, *Microwave Molecular Spectra*, John Wiley & Sons, 1984, p. 663.
36 M. J. Frisch, G. W. Trucks, H. B. Schlegel, G. E. Scuseria, M. A. Robb, J. R. Cheeseman, V. G. Zakrzewski, J. A. Montgomery, Jr., R. E. Stratmann, J. C. Burant, S. Dapprich, J. M. Millam, A. D. Daniels, K. N. Kudin, M. C. Strain, O. Farkas, J. Tomasi, V. Barone, M. Cossi, R. Cammi, B. Mennucci, C. Pomelli, C. Adamo, S. Clifford, J. Ochterski, G. A. Petersson, P. Y. Ayala, Q. Cui, K. Morokuma, N. Rega, P. Salvador, J. J. Dannenberg, D. K. Malick, A. D. Rabuck, K. Raghavachari, J. B. Foresman, J. Cioslowski, J. V. Ortiz, A. G. Baboul, B. B. Stefanov, G. Liu, A. Liashenko, P. Piskorz, I. Komaromi, R. Gomperts, R. L. Martin, D. J. Fox, T. Keith, M. A. Al-Laham, C. Y. Peng, A. Nanayakkara, M. Challacombe, P. M. W. Gill, B. Johnson, W. Chen, M. W. Wong, J. L. Andres, C. Gonzalez, M. Head-Gordon, E. S. Replogle and J. A. Pople, *GAUSSIAN 98 (Revision A.11.3)*, Gaussian, Inc., Pittsburgh PA, 2002.
37 A. A. Granowsky, http://classic.chem.msu.su/gran/gamess/index.html.
38 Z. Kisiel, *PROSPE – Programs for Rotational Spectroscopy*, http://info.ifpan.edu.pl/~kisiel/prospe.htm.
39 S. F. Boys and F. Bernardi, *Mol. Phys*., 1970, **19**, 55.
40 S. Simon, M. Duran and J. J. Dannenberg, *J. Chem. Phys*., 1996, **105**, 11024.
41 I. Alkorta, I. Rozas and J. Elguero, *Chem. Soc. Rev*., 1998, **27**, 163.
42 B. Raghavendra and E. Arunan, unpublished results.
43 C. J. Cramer, *Essentials of Computational Chemistry*, John Wiley and Sons, New York, 2002.
44 Z. Kisiel, B. A. Pietrewicz and L. Pszczólkowski, *J. Chem. Phys*., 2002, **117**, 8248.
45 T. D. Klots and H. S. Gutowsky, *J. Chem. Phys*., 1989, **91**, 63.
46 Y. Xu, M. C. L. Gerry, J. P. Connelly and B. J. Howard, *J. Chem. Phys*., 1993, **98**, 2735.
47 M. S. Ngarĩ and W. Jäger, *J. Chem. Phys*., 1999, **111**, 3919.
48 Z. S. Huang and R. E. Miller, *J. Chem. Phys*., 1989, **91**, 6613.

